ELSEVIER

Cryogenics 39 (1999) 739–750

Cryogenics

Hyperbolic heat conduction in thin-film high T_c superconductors with interface thermal resistance

Whey-Bin Lor, Hsin-Sen Chu *

Department of Mechanical Engineering, National Chiao Tung University, Hsinchu 300, Taiwan, ROC

Received 12 April 1999; accepted 30 June 1999

Abstract

This article numerically analyzes the hyperbolic heat conduction problem in the film and substrate composites under an imposed surface heat flux on the exterior film surface. The radiation heat flux model is employed to take account of the interface thermal resistance. The reflection and transmission occur at the contact surface of the dissimilar material which depends on the substrate properties and interface conditions. The interface resistance restricts the energy transmission across the interface and alerts the reflected and transmitted waves' strength. Neglecting the interface thermal resistance causes the temperature distribution in the film to be greatly underestimated. Moreover, the hyperbolic equation predicts significantly different results with those predicted by the parabolic equation at small time scales. The discrepancies between the solutions in an investigation of superconductor Y–Ba–Cu–O film depositions on several commonly used substrates are examined.

Keywords: High T_c superconductors (A); Heat transfer (C)

Nomenclature

$[A]$	Jacobian matrices
c	thermal wave speed
C_p	specific heat capacity
$\boldsymbol{F}$	flux vector, defined in Eq. (11)
$\boldsymbol{G}$	source vector, defined in Eq. (21)
H	Heaviside's unit function
h	Planck's constant
k	thermal conductivity
k_B	Boltzmann constant
$\boldsymbol{M}$	flux vector, defined in Eq. (21)
q	heat flux
$\boldsymbol{q}$	heat flux vector
$\boldsymbol{r}$	position vector
$[R]$	right eigenmatrix, defined in Eq. (16)
Q	total energy
$\boldsymbol{S}$	source vector, defined in Eq. (11)
t	time
T	temperature
T_o	operating temperature
t_p	duration time
$\boldsymbol{U}$	unknown vector, defined in Eq. (11)
$\bar{v}$	sound velocity
W	characteristics variable
$\boldsymbol{W}$	characteristics vector, defined in Eq. (21)
x	position

Greek symbols

ρ	density
α	thermal diffusivity
τ	relaxation time
λ	eigenvalue
κ	constant; see Eq. (5)
Γ	constant; see Eq. (5)

Superscripts

$n, n+1$	time levels n and $n+1$
iter	iteration

Subscripts

j	media index, 1 represent film; 2 represent substrate
c	interface
i	control volume index
$i \pm 1/2$	value at control volume faces
xo	film surface ($x = 0$)

* Corresponding author. Tel.: +886-3-571-2121 ext: 55115; fax: +886-3-572-7930.

E-mail address: hschu@cc.nctu.edu.tw (H.-S. Chu)

0011-2275/99/$ - see front matter
PII: S0011-2275(99)00085-5

1. Introduction

Since the discovery of high-temperature superconductors, a variety of electronic devices have used a thin film of superconducting material deposited on a substrate. The typical examples are Josephson junctions and superconducting bolometers. During the operation of superconducting detectors, the heat is incident on the surface of the film and increases the film temperature. If the temperature is higher than the transition level, the superconductors may change from the superconducting state to the normal resistive state. Therefore, understanding the temperature distribution in practical superconducting film and substrate composites is a relevant task.

In modeling the heat transfer behavior of a superconducting detector subject to incident energy, the diffusion theory (Fourier law) has generally been utilized [1–5]. The traditional heat conduction equation implies that the heat propagates at an infinite speed. Despite such an unacceptable notion of energy transport in solids, the classical Fourier law yields reliable results for most circumstances, mainly because the thermal diffusivity is ten orders of magnitude smaller than that corresponding to the speed of a thermal wave in most situations. Nevertheless, with the advent of science and technology involving the conditions of cryogenic temperature, short duration, high-rate change of temperature or heat flux, the assumption of infinite thermal propagation speed might not be sufficiently accurate. Some investigations have indicated that the heat propagation velocity under such circumstances becomes finite and dominant [6–9]. The operation of the superconducting detectors can be based on cryogenic temperature, thin thickness, and short duration of high-rate heat flux change. The finite speed of heat propagation may have to be considered in modeling the heat transfer in these devices.

While considering the finite speed of wave propagation, Cattaneo [10] and Vernotte [11] independently suggested a modified heat flux model in the form of

$$\boldsymbol{q}(\boldsymbol{r}, t+\tau) = -k\nabla T(\boldsymbol{r}, t), \tag{1}$$

where τ is the relaxation time, k the thermal conductivity, $\boldsymbol{r}$ the position vector, and t is the physical time. Clearly, for $\tau = 0$, Eq. (1) reduces to the classical diffusion theory, leading to an infinite propagation velocity. In addition, when Eq. (1) is used in a local energy balance, a hyperbolic equation is obtained. Temperature fields obtained from the hyperbolic heat conduction equation often display wavelike characteristics that would not be predicted by the parabolic type traditional diffusion theory [12]. Several investigators have estimated and predicted the magnitude of τ for engineering material [13–18]. In the superconducting state, heat is transferred predominately by phonons, with phonon velocity of the order of 10^3 m/s [19,20]. This value is further smaller than that in metals, which predominantly transfer heat due to electrons, with thermal propagation speed of the order of 10^6 m/s. Based on the kinetic theory [13] , the relaxation time τ for YBaCuO film is $\approx 300, \approx 0.6, \approx 0.4$ ps for $T = 4$, 50 and 77 K, respectively. Recently, Mitra et al. [21] determined experimentally the τ value to be approximately 16 s for a biological material and directly validated the hyperbolic natural of heat conduction by comparing the temperature with the non-Fourier predictions.

While emphasizing engineering applications of the thermal wave theory, Özisik and Tzou [22] thoroughly reviewed thermal wave propagation, including the sharp wave front and rate effects, thermal shock phenomenon, thermal resonance phenomena, and reflection and refraction of thermal waves across a material interface. Tzou [23] further proposed a general criterion for the dominance of wave behavior over diffusion

$$\frac{\partial T}{\partial t} \gg \left\{ \frac{T_o c^2}{2\alpha} \exp\left(\frac{c^2 t}{\alpha}\right) \right\} \tag{2}$$

with T_o being the reference temperature. According to this criterion, relative importance of the wave behavior in heat conduction can be examined by considering the interaction of three factors which contained the thermal properties (α and c), the thermal loading and response conditions ($\partial T/\partial t$ and T_o) and the transient time (t). If the heat transfer process occurs in an extremely short period of time or that with an extremely high rate of temperature increase, the wave behavior may become pronounced regardless of the value of T_o. In experiments to investigate the non-equilibrium response mechanism, heating pulses can be as short as the order of a picosecond with the heat flux value up to the order of 10^9–10^{11} W/m^2 [24,25]. This high heat flux value is further larger than that of the critical value of 10^7 W/m^2 for the Fourier heat flux model breaking down [7].

By applying the thermal wave model, there are several investigations concerning the heat transfer behavior in the thin film, which might possibly be the case for the operation of certain thin film superconducting devices. Those works include the step change of boundary heat flux [26–28], boundary temperature jump [29–31], oscillatory boundary heat input [32–34], and the impulse heat pulse [35–38]. It is found that the temperature predicted by hyperbolic equation is significantly higher than that predicted by Fourier's law. The previous investigations deal with the bare film structure, i.e. ignored the substrate effect. Frankel et al. [39] proposed a flux formulation to investigate the thermal waves in a two-layer composite media with perfect contact interface. The internal reflections are produced at the interface of two dissimilar media and the thermal properties ratio of different layers significantly influence the heat transfer

solutions in the composite media. In addition to being influenced by the thermal properties of the substrate, the heat transfer behavior in the film is also heavily influenced by the interface thermal resistance at the contact surfaces of film with the substrate in the Fourier's low analysis [1–4,25]. However, the influence of interface thermal resistance on the hyperbolic heat conduction has not been investigated yet to date.

To consider the thermal boundary resistance at the contact interface of two dissimilar materials, the radiation-boundary-condition at the interface where the thermal flow across the interface proportional to the difference of the fourth power of the temperature on each side of the interface is employed [40,41]. Taking the most common substrates used for Y–Ba–Cu–O film (MgO, $SrTiO_3$, $LaAlO_3$, and sapphire), the influences of the substrates and interface thermal resistance are examined in this study. Results demonstrate that the effect of the substrate, interface resistance and surface heat pulse duration can be very important to the heat transfer in a thin-film superconductor deposited on substrates as predicted by hyperbolic and parabolic heat conduction equations.

2. Physical model and theoretical analysis

The constitutive and energy conservation equations used in the thermal wave theory take the form [12]

$$q(x,t)+\tau\frac{\partial q(x,t)}{\partial t}=-k\nabla T(x,t) \tag{3a}$$

and

$$\rho C_{\mathrm{p}}\frac{\partial T(x,t)}{\partial t}+\nabla\cdot q(x,t)=0. \tag{3b}$$

The physical system under consideration is shown in Fig. 1. A thin-film superconductor of thickness x_1 is deposited on a substrate. The film and substrate are initially at the same temperature as the coolant of T_{o}. At $t=0^+$, a step change of constant heat flux is imposed at the exterior surface of the film for the duration t_{p} where $H(t)$ is the Heaviside's unit function. The heat flux q_{o} can be thought of as the net heat flux into the film, e.g., for a detector, the difference between the incident radiation and any losses from the surface to the surroundings. In addition, the back surface of the substrate at $x=x_2$ is maintained at the coolant temperature of T_{o}. To predict the thermal resistance at the interface of the film and substrate, a radiation-boundary-condition model is employed. This obtains [40, 41]

$$q_c=\kappa(T_{1c}^4-T_{2c}^4)\ \text{at the interface}, \tag{4}$$

where

$$\kappa=\frac{2\pi k_{\mathrm{B}}^4\Gamma}{h^3\bar{v}^2}\left(\frac{\pi^4}{15}\right). \tag{5}$$

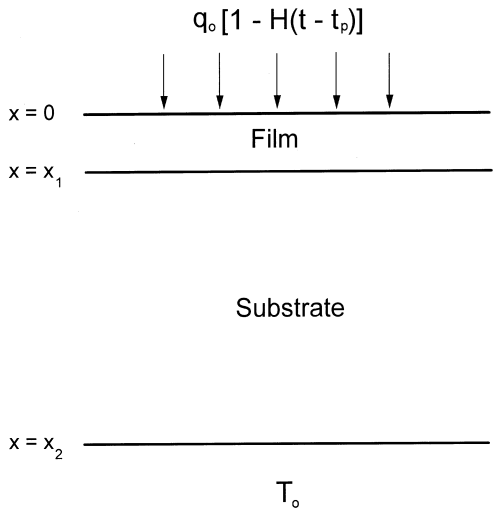

Fig. 1. The physical model of a thin-film superconductor deposited on a substrate.

The most important constant is Γ, a function of the material properties of the two media in contact. Using the figure provided by Little [40], Γ can be obtained if the density ratio and the sound velocity ratio of the two media are known. The higher Γ (or κ) value represents higher transmission across the interface, i.e. a lower interface thermal resistance.

For convenience, in the subsequent analysis, the non-dimensional variables are defined in the transformed system as follows:

$$x^*=\frac{c_1x}{2\alpha_1},\quad t^*=\frac{c_1^2t}{2\alpha_1},\quad T_j^*=\frac{T_j}{T_{\mathrm{o}}},\quad q_j^*=\frac{\alpha_1q_j}{T_{\mathrm{o}}k_1c_1},\quad \kappa^*=\frac{\kappa T_{\mathrm{o}}^3\alpha_1}{k_1c_1} \tag{6}$$

and the dimensionless property ratios

$$\alpha_j^*=\frac{\alpha_j}{\alpha_1},\quad \tau_j^*=\frac{\tau_j}{\tau_1},\quad k_j^*=\frac{k_j}{k_1}, \tag{7}$$

where c represents the thermal wave speed and equals $(\alpha/\tau)^{1/2}$. The subscripts $j=1$, and 2 represent the film and substrate, respectively. Clearly, we have $\alpha_1^*=\tau_1^*=k_1^*=1$. The energy equation and non-Fourier constitutive equation are expressed in terms of the above dimensionless variables as (with asterisks omitted)

$$\frac{\partial T_j}{\partial t}+\frac{1}{k_j}\frac{1}{\alpha_j}\frac{\partial q_j}{\partial x}=0, \tag{8}$$

$$\frac{\partial q_j}{\partial t}+\frac{k_j}{\tau_j}\frac{\partial T_j}{\partial x}=-2\frac{1}{\tau_j}q_j. \tag{9}$$

The non-Fourier constitutive equation along with the energy equation for the film and substrate can be written in dimensionless vector form as

$$\frac{\partial \boldsymbol{U}_j}{\partial t}+\frac{\partial \boldsymbol{F}_j}{\partial x}=\boldsymbol{S}_j, \tag{10}$$

where

$$\boldsymbol{U}_j = \begin{Bmatrix} T_j \\ q_j \end{Bmatrix}, \quad \boldsymbol{F}_j = \begin{Bmatrix} \frac{1}{k_j}\frac{1}{\alpha_j} q_j \\ \frac{k_j}{\tau_j} T_j \end{Bmatrix}, \quad \boldsymbol{S}_j = \begin{Bmatrix} 0 \\ -2\frac{1}{\tau_j} q_j \end{Bmatrix}. \tag{11}$$

Eq. (10) can be written as

$$\frac{\partial \boldsymbol{U}_j}{\partial t} + [A]_j \frac{\partial \boldsymbol{U}_j}{\partial x} = \boldsymbol{S}_j \tag{12}$$

and the Jacobian matrices are

$$[A]_j = \frac{\partial \boldsymbol{F}_j}{\partial \boldsymbol{U}_j}. \tag{13}$$

Then, $[A]_j$ can be diagonalized through the eigenvectors

$$[A]_j = [R]_j [\lambda]_j [R]_j^{-1}, \tag{14}$$

where λ denotes the diagonal matrices consisting of two eigenvalues of $[A]$ for each layer. The superscript -1 represents the inverse eigenmatrix. The diagonal matrices and the right eigenmartices show that

$$[\lambda]_j = \begin{bmatrix} -\left(\frac{\alpha_j}{\tau_j}\right)^{1/2} & 0 \\ 0 & \left(\frac{\alpha_j}{\tau_j}\right)^{1/2} \end{bmatrix}, \tag{15}$$

$$[R]_j = \begin{bmatrix} 1 & 1 \\ -k_j\left(\frac{1}{\alpha_j}\frac{1}{\tau_j}\right)^{1/2} & k_j\left(\frac{1}{\alpha_j}\frac{1}{\tau_j}\right)^{1/2} \end{bmatrix}. \tag{16}$$

In addition, the dimensionless interface condition is in the form of

$$q_{1c} = q_{2c} \quad \text{and} \quad T_{1c} = T_{2c} \quad \text{for perfect contact interface,} \tag{17a}$$

$$q_{1c} = q_{2c} = \kappa[(T_{1c})^4 - (T_{2c})^4] \quad \text{for interface with thermal resistance.} \tag{17b}$$

The dimensionless initial conditions are given as

$$T = 1 \quad \text{and} \quad q = 0, \qquad \text{at } t = 0. \tag{18}$$

At $t > 0$, a constant heat flux with dimensionless value of unity is imposed at the exterior surface of the film for a duration of t_p. After the pulsed duration, the film surface condition is assumed to be adiabatic. In addition, the back surface of the substrate cooled by the coolant is maintained at the initial or operating temperature T_o. The boundary conditions become

$$q = \begin{cases} 1, & t < t_p \\ 0, & t > t_p, \end{cases} \quad \text{at } x = 0, \tag{19a}$$

$$T = 1 \quad \text{at} \quad x = x_2. \tag{19b}$$

3. Numerical method

This study uses the characteristics-based numerical method developed by Yang [42] which resolves the thermal wave without introducing oscillation or dissipation, to solve the system of equations. First, multiply Eq. (12) by $[R]_j^{-1}$, then obtain

$$\frac{\partial \boldsymbol{W}_j}{\partial t} + \frac{\partial \boldsymbol{M}_j}{\partial x} = \boldsymbol{G}_j, \tag{20}$$

where

$$[W]_j = [R]_j^{-1} \cdot [U]_j [M]_j = [\lambda]_j \cdot [W]_j \qquad [G]_j = [R]_j^{-1} \cdot [S]_j. \tag{21}$$

Now, the problem attempts to solve the characteristics variable $[W]$, instead of the original T and q coupled equation. Then, Eq. (20) is expanded by the finite difference and explicit methods, therefore, we have

$$\boldsymbol{W}_i^{\text{iter}} = \boldsymbol{W}_i^n - \frac{\Delta t}{\Delta x}\left(\boldsymbol{M}_{i+1/2}^n - \boldsymbol{M}_{i-1/2}^n\right) + \Delta t \boldsymbol{G}_i^{\text{iter}}, \tag{22}$$

where $\Delta x = x_{i+1/2} - x_{i-1/2}$ and $\Delta t = t^{n+1} - t^n$. The superscript iter denotes the iteration value at new time step of $n+1$.

The total variation diminishing scheme [42] is used to compute the characteristic variable $[W]$ of the interior points. Moreover, a simple and accurate numerical algorithm presented by Yeung and Lam [43] applying the Godunov method is employed to compute the $[W]$ value at the point next to the boundaries.

The interface temperatures of the film and substrate (T_{1c} and T_{2c}) at time step n are used to calculate the interface heat flux (q_c) for time step $n+1$. Based on this interface heat flux, the new iteration T and q values of the film are obtained. The interface heat flux is updated by the new iteration value of T_{1c}. Then, based on the updated q_c, new iteration T and q values of the substrate are obtained. The procedure is repeated until the T and q in the film and substrate composites are valid for the criterion of convergence

$$\left|\frac{T - T^{\text{iter}}}{T}\right|_{\max} \leqslant 10^{-5} \quad \text{and} \quad \left|\frac{q - q^{\text{iter}}}{q}\right|_{\max} \leqslant 10^{-5}. \tag{23}$$

Then, the new values of T and q of the film and substrate at the time $n+1$ can be evaluated.

4. Results and discussion

A one-dimensional computer code was written on the basis of the above calculation procedure. Grid refinement and time step sensitivity studies have also been performed for the physical model to ensure that the essential physics are independent of grid size and time interval. Typically, the substrate thickness is several 100 or even 1000 times thicker than the thin film. A film with

a dimensionless thickness of 0.5 deposited on the substrate with a dimensionless thickness of 30 is considered in this study.

4.1. Perfect contact interface

Figs. 2 and 3 display the influence of the thermal properties of the substrate on the heat flux and temperature distribution, respectively, in the film and partially in the substrate, using the thermal wave heat transfer model. The film surface heat flux duration t_p is 1. The bare film solution which neglects the effect of the substrate and a prescribed constant temperature T_o of the coolant at the back surface of the film [28], is presented as a reference to enable an understanding of the substrate effect. The hyperbolic wave nature is clearly shown by displaying the sharp wave front, and an undisturbed region ahead of its front. The wave front located at $x = 0.2$ at $t = 0.2$ since the dimensionless wave speed in the film is unity. By effect of diffusion, a slant across the top of the wave is observed. The hyperbolic heat conduction equation predicts that a thermal wave disturbance tends to propagate in a given direction with a propagation speed of c until its course is impeded by a wall or barrier. Therefore, before the wave front impacts the interface at $x = 0.5$, the heat flux and temperature distribution is identical for each different substrate property and bare film solution, as attributed to the fact that the wave front is unaware of the existence of the substrate. The substrate effect is clearly illustrated after the wave front has encountered the interface. By $t = 0.6$, the internal reflection and transmission occur at the contact surface of the dissimilar material. The reflected wave fronts move toward the exterior surface of the film, and the transmitted waves toward the exterior surface of the substrate. The higher substrate conductivity represents the higher heat transfer ability to transmit energy when the wave front has an impact on the interface. In

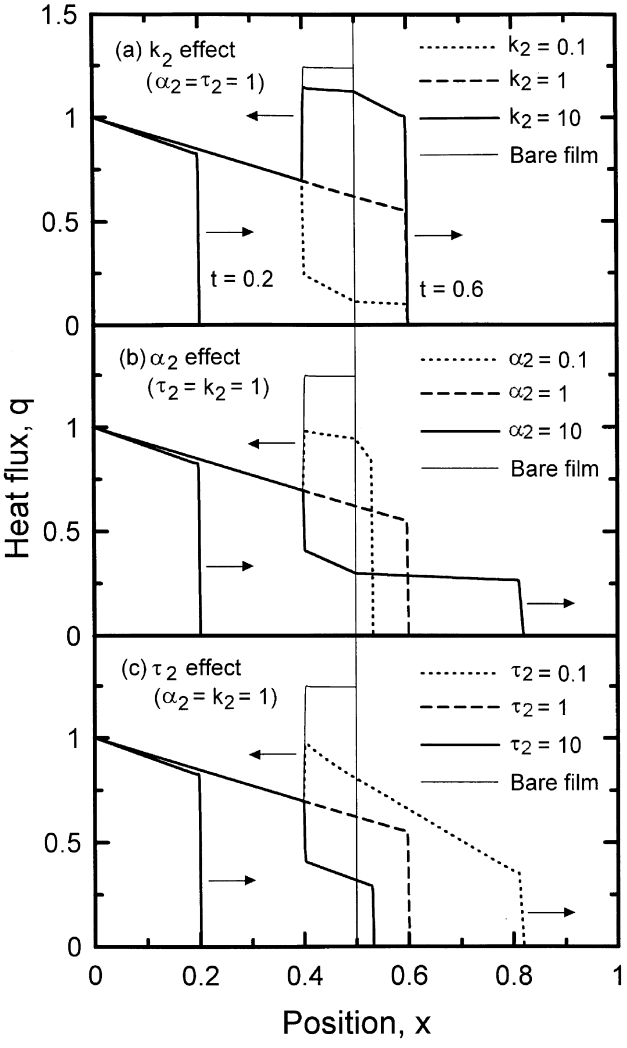

Fig. 2. Influence of substrate properties on hyperbolic heat flux distributions in the film and partially in substrate with $t_p = 1$.

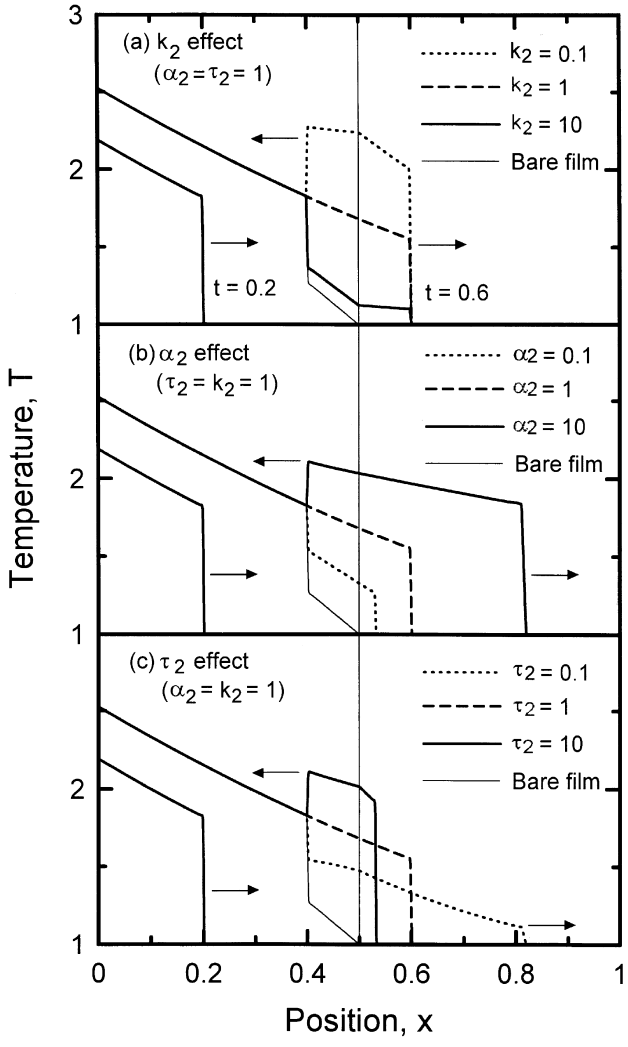

Fig. 3. Influence of substrate properties on hyperbolic temperature distributions in the film and partially in substrate with $t_p = 1$.

addition, the heat capacity of symbol ρC_p changes proportionally to k when α is held constant. Thus, the effect of substrate conductivity tends to increase the heat flux profiles but decrease the temperature profiles as k_2 increases (Figs. 2a and 3a). Moreover, since the wave speed in the film and substrate is the same when $\alpha_2 = \tau_2 = 1$, the wave fronts coincides, regardless of the conductivity value. However, the wave speed in the substrate is varied with α_2 and α_2, since $c_2 = (\alpha_2/\tau_2)^{1/2}$. When $\alpha_2 > \alpha_1$ with $\tau_2 = \tau_1$, the wave travels in the substrate faster than in the film. This difference in wave speed leads to the transmitted wave in the substrate being pulled away faster than the reflected wave in the film (Figs. 2b and 3b). The opposite occurs when $\alpha_2 < \alpha_1$. Moreover, as α_2 increases, substrate diffusivity tends to decrease the heat flux profiles but increase the temperature profiles, as attributed to the fact that the heat capacity of ρC_p changes inversely proportional to α when k is held constant. In Figs. 2c and 3c, the transmitted wave front is stretched when the relaxation time of the substrate is smaller than that of the film. In addition, the lower relaxation time of the substrate leads to the higher heat flux and lower temperature profile. The influence of the substrate properties on the internal reflections and transmissions heat flux and temperature are analogous with the research for analysis by Frankel et al. [39] in finite composite media exposed to a pulsed volumetric source. It is clearly demonstrated that the heat flux and temperature in the film are heavily influenced by the substrate. Furthermore, the temperature in the film is markedly underestimated when using bare film approximation.

Fig. 4 presents the interface heat flux and temperature for various substrate properties, to illustrate the validity of bare film approximation. The values present in Fig. 4 are taken at $t = 0.6$ after the interaction of the wave front with the interface. The interface heat flux goes to zero, which indicates that no heat flux is transferred through the interface into the substrate when the substrate conductivity k is less than 10^{-2}, or α or τ is greater than 10^4. Meanwhile, this results in high interface temperature. In contrast, when k is greater than 10^2 or α is less than 10^{-4}, the substrate effect can be neglected and the interface temperature equals to the coolant temperature of T_o. This indicates that the heat transfer ability of the substrate approaches an infinite value and results in the heat flux at the interface approaching a limiting high value. Notably, there is no critical τ_2 value to approach the bare film approximation. From Eq. (1), the heat wave model allows a time lag between the heat flux and the temperature gradient. The relaxation time τ is associated with the communication time between phonons (phonon–phonon collisions) that is necessary before commencing heat flow. When the relaxation time of the substrate increases, the commencement of the heat flow is delayed and the temperature accumulates. Thus,

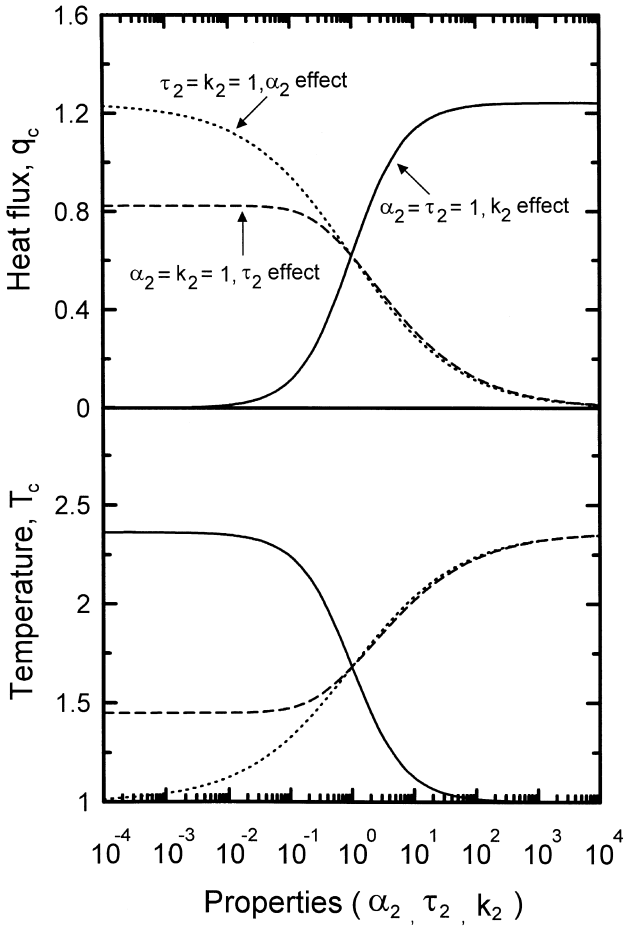

Fig. 4. Influence of substrate properties on hyperbolic interface heat flux and temperature to demonstrate the validity of bare film approximation.

the temperature increases with an increase of τ_2; conversely, the heat flux decreases with an increase of τ_2. In contrast, when τ_2 is sufficiently low, the commencement of the heat flow will not be delayed and will act more like the Fourier's diffusion heat transfer model. Then, the limiting heat flux and temperature values are found to be independent of the variation in the relaxation time of the substrate. These limiting values cannot be obtained from the bare film structure.

Bai and Lavine [28] investigated the importance of the finite thermal propagation speed in the bare film with a prescribed temperature at the back surface of the film for directing application to thin film high temperature superconducting electronic devices. However, according to Figs. 2–4, the assumption of ignored substrates is inappropriate, except for special substrate properties. To investigate the effect of the substrate on the heat transfer in superconducting devices in this study, a typical system was chosen consisting of a Y–Ba–Cu–O film deposited on the four most common substrates in use: $LaAlO_3$, MgO, $SrTiO_3$, and sapphire. The properties of the film and substrates at the initial temperature

Table 1
Characteristic parameters of Y–Ba–Cu–O film, substrates at operating temperature of 77 K

T_o (K)	k_1[a] (W/mK)	ρ_1[a] (kg/m^3)	$C_{p,1}$[a] (J/kg K)	Substrate	α_2/α_1	τ_2/τ_1[b]	k_2/k_1	Γ[c]
77	2.2	6350	156	$LaAlO_3$[d]	100	50	10	0.3
				Sapphire[e]	2000	800	500	0.2
				MgO[a]	1000	200	200	0.2
				$SrTiO_3$[e]	10	2	10	0.15

[a] [1].
[b] [13].
[c] [40].
[d] [44].
[e] [45].

of 77 K are listed in Table 1. Fig. 5 illustrates the temperature distribution in the film and partially in substrates, at $t = 0.2$ and 0.7, as predicted by the hyperbolic and parabolic equations. In Fig. 5a, the parabolic solution shows a continuous temperature distribution, which is in contrast to the normal nature of hyperbolic waves. The diffusion model predicts that the temperature profile is dependent on the used substrate at $t = 0.2$, as the result of the infinite propagation speed. A high thermal conductivity conducts heat more rapidly to the coolant and thus reduces the temperature increment in the film. Thus, the lowest temperature is obtained by using the sapphire substrate. The effect of diffusivity is clearly shown by comparing the solutions of $LaAlO_3$ and $SrTiO_3$ (because the difference in their diffusivity is 10 times, while their thermal conductivity is the same). The temperature distribution is highest for $LaAlO_3$, as a result of its low conductivity and high diffusivity. According to Fig. 5b, the hyperbolic temperature profile was affected by the substrate at $t = 0.7$ after the wave front impact on the interface. Nevertheless, in the thermal wave model, the heat transfer behavior is not only mediated by the conductivity and diffusivity, but also by the relaxation time of the substrate. A comparison of the properties of $LaAlO_3$ and $SrTiO_3$ shows that their thermal conductivity is equal and low, however, the $LaAlO_3$ exhibits the highest temperature profile; conversely, $SrTiO_3$ exhibits the lowest temperature profile in the four different substrates, because of the differences in their diffusivity and relation time.

Fig. 6 depicts the average film temperature as time elapses for different substrates. For the hyperbolic solution, there is no heat transfer across the interface prior to the impact of the wave front on the interface. Thus, the hyperbolic average film temperature remains constant and is independent of the substrate for $t < 0.5$. Subsequently, the average temperature abruptly drops to a value that depends on the used substrate when the leading edge of the wave front impacts the interface at $t = 0.5$. The discontinuity behavior occurs after a dimensionless time interval of 1 when the waves reflected by the film surface impact the interface again until they have become damped out by the effect of diffusion and energy transmitted into the substrate. For the remaining time, when the waves do not impact the interface, the average film temperature gradually changes with time; this is attributed to the exchange of a slight amount of energy across the interface by the residual energy in the wake of propagating wave. It is clearly shown that the hyperbolic model predicts higher temperatures at small time scales than those predicted by the parabolic model. The difference between the predictions of the two models diminishes with time. For bare film approximation, and high conductivity materials such as sapphire and MgO, the solutions obtained for both models coincide and are in a steady state after a dimensionless time greater than

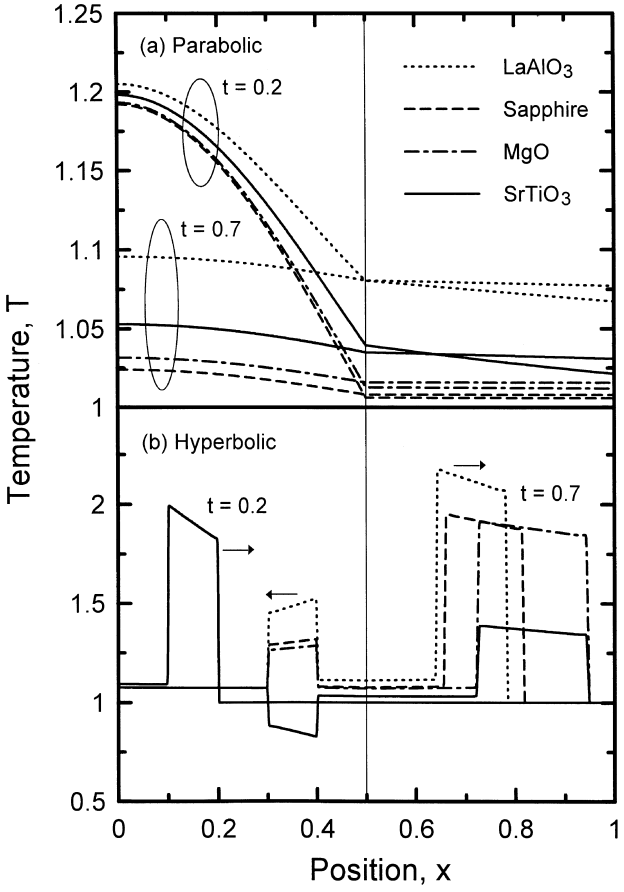

Fig. 5. Comparison of parabolic and hyperbolic temperature distribution in the film and partially in substrates with $t_p = 0.1$.

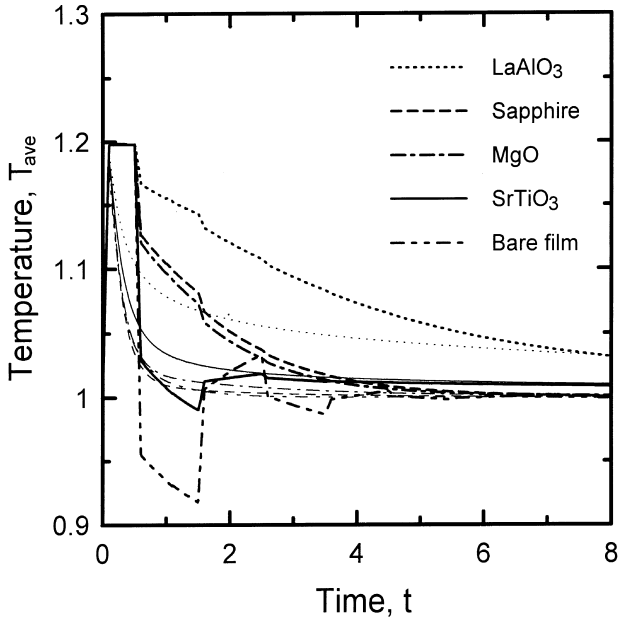

Fig. 6. Comparison of parabolic and hyperbolic average film temperature versus time with $t_p = 0.1$. The light and dark lines represent the parabolic and hyperbolic solutions, respectively.

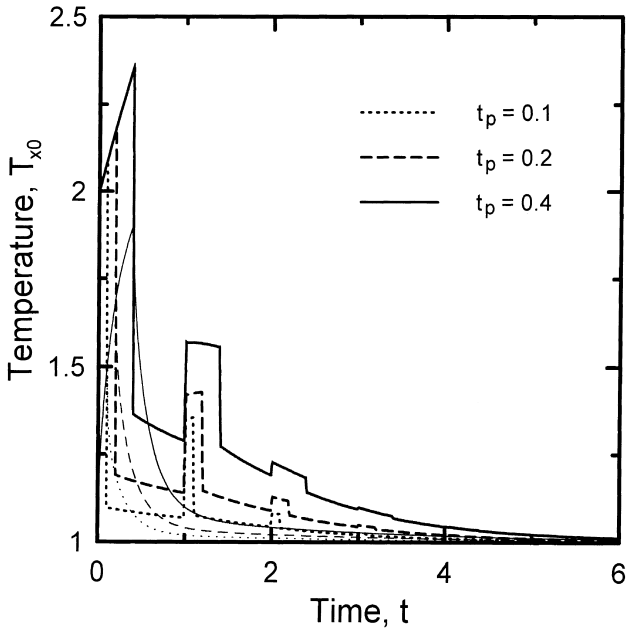

Fig. 7. Comparison of parabolic and hyperbolic film surface temperature versus time with various duration for substrate MgO. The light and dark lines represent the parabolic and hyperbolic solutions, respectively.

about 5. Nevertheless, using substrates $LaAlO_3$ and $SrTiO_3$ requires longer time scales than using other substrates, for the solutions obtained from parabolic equation coincides with that for the solutions obtained from the hyperbolic equation.

Fig. 7 depicts the film surface temperature as time elapses when the film is deposited on the substrate MgO with various duration values. The parabolic solution shows that a smooth variation of temperature with time within the duration interval is a result of the instantaneous heat diffusion. In contrast, the hyperbolic equation gives rise to an infinite slope to increase the surface temperature from 1 to 2, in response to all the imposed heat energy concentrated on this surface at $t = 0^+$. Then, the temperature continuously increases for a period equal to the duration. This phenomenon might change the superconductors from the superconducting state to the normal resistive state, especially with a longer heat pulse duration. In addition, more energy is incident into the film for a longer duration, thus, the time taken is longer to damp out the nature of the wave of the hyperbolic solution by the effect of diffusion and energy transmitted into the substrate.

4.2. Interface thermal resistance

Fig. 8 illustrates the dimensionless total energy in the film as time elapses, when the film is deposited on the sapphire substrate under various interface conditions. The dimensionless total energy Q_1 can be obtained from the spatial integral of $\rho C_p T$ in the entire area of the film.

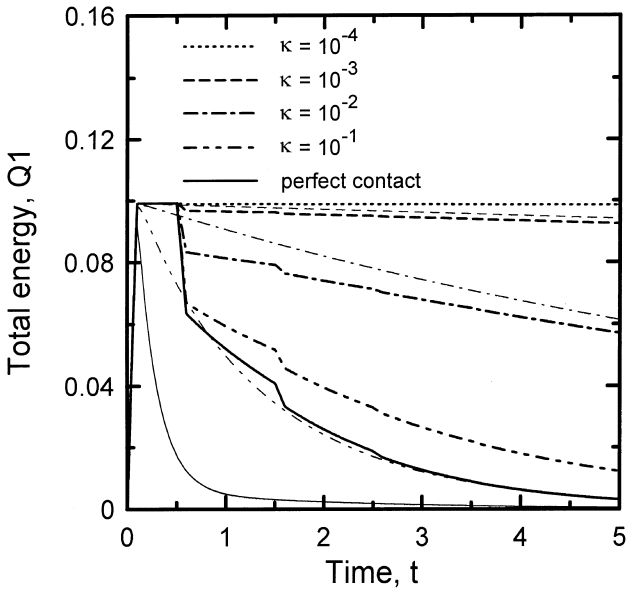

Fig. 8. Comparison of parabolic and hyperbolic film total energy versus time with various interface condition for substrate sapphire with $t_p = 0.1$. The light and dark lines represent the parabolic and hyperbolic solutions, respectively.

The higher κ value represents the higher transmission across the interface, i.e. a lower interface resistance. For hyperbolic solutions, the interface resistance effects an obvious variation in Q_1 when $t > 0.5$. The energy is restricted to transmit across the interface when thermal resistance exists. When the dimensionless resistance

constant κ (which represents the interface resistance magnitude) is less than the order of 10^{-3}, the total energy Q_1 nearly remain at the constant value of 0.1. The value equals the total incident energy, indicating that there is almost no heat transfer across the interface to the substrate, and the interface is equivalently adiabatic. In addition, when the interface resistance magnitude is in the order of 10^{-1}, the discrepancy from the perfect contact interface is relatively minor. It is clearly demonstrated that when the interface resistance is ignored, the Q_1 value, which can represent the average film temperature is significantly underestimated. Notably, the solution discrepancies between hyperbolic and parabolic significantly depends on the interface condition. For parabolic solutions, when the interface is in perfect contact or κ is in the order of 10^{-1}, the heat easily diffuses across the interface into the substrate instantaneously. That results in the hyperbolic solution being higher than predicted by the parabolic equation in the presented time domain. On the other hand, because the heat diffusion into substrate is small when the interface with κ is less than 10^{-2}, it causes the minor parabolic Q_1 to decrease with time. In addition, because the heat transfer across the interface is proportional to the difference of the fourth power of temperature on each side of the interface, the energy concentration occurring at the wave front in the hyperbolic type transfers more heat across the interface than in the parabolic type at $t = 0.5$. This event accounts for why the hyperbolic solutions are lower than the parabolic solutions when κ is in the order of 10^{-2}. When κ is in the order of 10^{-3} and 10^{-4}, nearly equivalent to the adiabatic interface condition, the solutions obtained from both heat transfer models almost coincides. From the figure provided by Little [40], the Γ value for Y–Ba–Cu–O deposited on the sapphire substrate is about 0.2, which corresponds to the dimensionless resistance magnitude κ in the order of 10^{-3}. This value indicates that the thermal resistance of the interface should be considered. In addition, the dimensionless resistance magnitude κ is in the same order of 10^{-3} for each of the four different substrates, as listed in Table 1. With this interface resistance magnitude, the effects of the substrates are as demonstrated in Figs. 9 and 10.

Fig. 9 clearly reveals that only a small amount of energy can be transferred across the interface with a resistance magnitude of $\kappa = 10^{-3}$ for all four substrates. This indicates that the interface acts more like an adiabatic interface condition. Thus, the temperature profile in the film is independent of the used substrates for both hyperbolic and parabolic equations, despite the different properties among those substrates. Moreover, the temperature continuity condition at the interface breaks down. The temperature jump at the interface is attributed to the increment of film temperature, and the reduction of the substrate temperature from the perfect

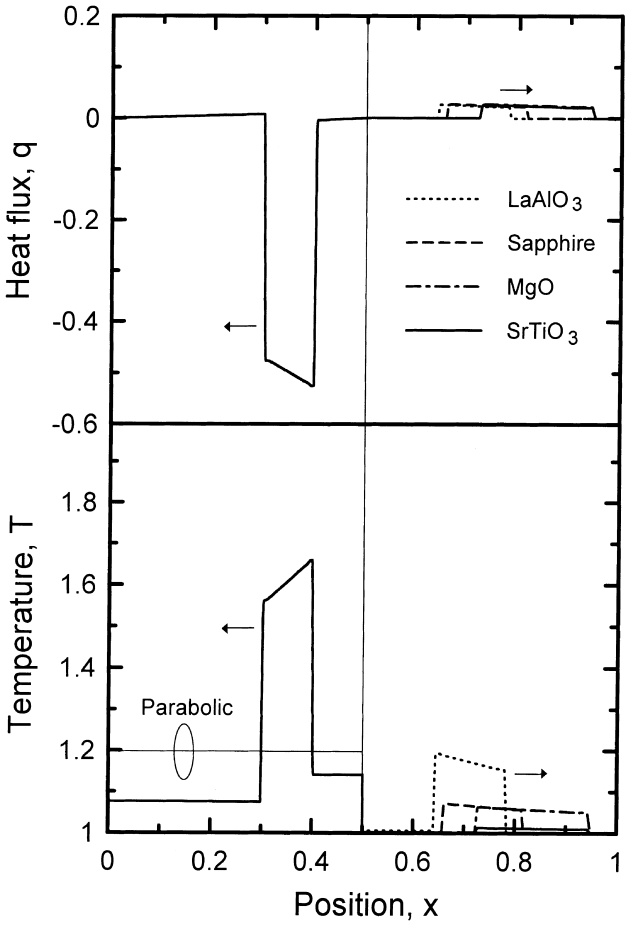

Fig. 9. Temperature distribution in the film and partially in substrates with interface resistance and $t_p = 0.1$.

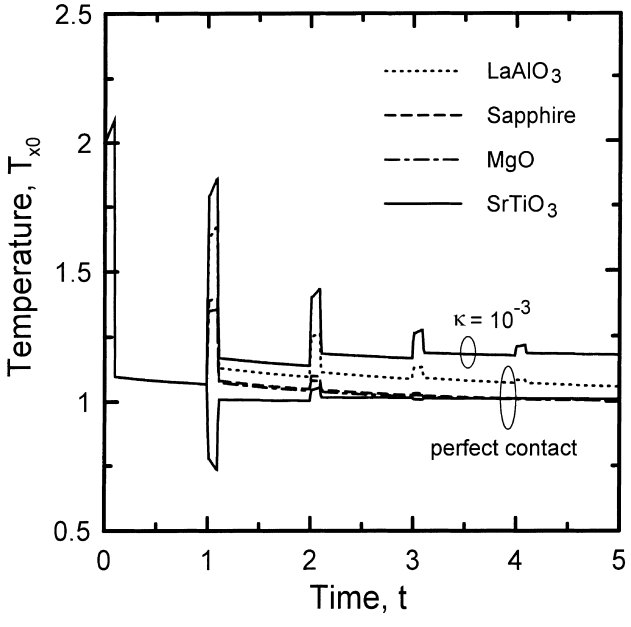

Fig. 10. Comparison of film surface temperature versus time between perfect contact interface and resistance interface with $t_p = 0.1$.

contact value. The temperature profile in the substrates is dependent on the substrate for their different heat capacity of symbol ρC_p, corresponding with the small amount of energy transmitted into the substrate. This substrate temperature dependence causes the heat transfer across the interface to vary with the deposited substrate while the wave reflected by the film surface impacts the interface again for a longer duration, as presented in Fig. 11.

Fig. 10 illustrates the film surface temperature discrepancies between the perfect contact and the resistance interface for the four substrates. The energy restricted in the film caused by the resistance interface is more than that caused by the perfect contact interface. Therefore, when the interface is in resistance condition, the time to damp out the hyperbolic wave nature takes longer than that in perfect contact condition. In addition, higher film surface temperature is predicted for the interface with thermal resistance. Due to the substrate $SrTiO_3$ exhibits the highest temperature in the perfect contact condition, the discrepancies between the different interface conditions for substrate $SrTiO_3$ is less significant than others. Despite the significant deviation among various substrates with perfect contact interface, the values are nearly the same when $\kappa = 10^{-3}$. This virtual equivalence indicates that when the thermal resistance is considered, the heat transfer behavior in the Y–Ba–Cu–O film is almost independent of the four substrate deposits at this duration value. Nevertheless, the substrate dependence on the interface heat transfer is observed for longer duration, as presented in Fig. 11. When the leading edge of the initial wave front impacts the interface at $t = 0.5$, the interface heat flux abruptly increases from zero to a value that is independent of the substrate and duration. Thereafter, the energy concentrates in the wave width causing the interface heat flux to gradually increase with time. At $t = 1.5$, the waves reflected by the film surface impact the interface again. At this moment, the temperature of the wave front is dependent on the heat duration. The wave reflected by the interface is heated by the film surface when the duration is greater than unity. This heating causes the temperature at the wave front at $t = 1.5$ to be much higher than that at $t = 0.5$. In addition, the heat flux across the interface is proportional to the difference of the fourth power of temperature on each side of the interface for a constant κ value. Therefore, at this moment, the energy crosses the interface easier than $t = 0.5$, and the interface acts less like an adiabatic condition. Moreover, the interface film temperature is equal for different substrates, however, the interface substrate temperature depends on the substrate. Therefore, the heat transfer dependence is observed for $t > 1.5$ when duration is greater than unity. The heat transfer across the interface for $LaAlO_3$ is less than other substrates; this is attributed to the temperature in this substrate being higher than in other substrates. This poor heat transfer ability produces the longer time required for substrate $LaAlO_3$ to approach the steady state.

Fig. 12 illustrates the difference between Q_1 obtained from hyperbolic and parabolic equations as a function of time with the varied duration. The solution discrepancies between the parabolic and hyperbolic equations are observed for time greater than 2 at $t_p = 10$. This

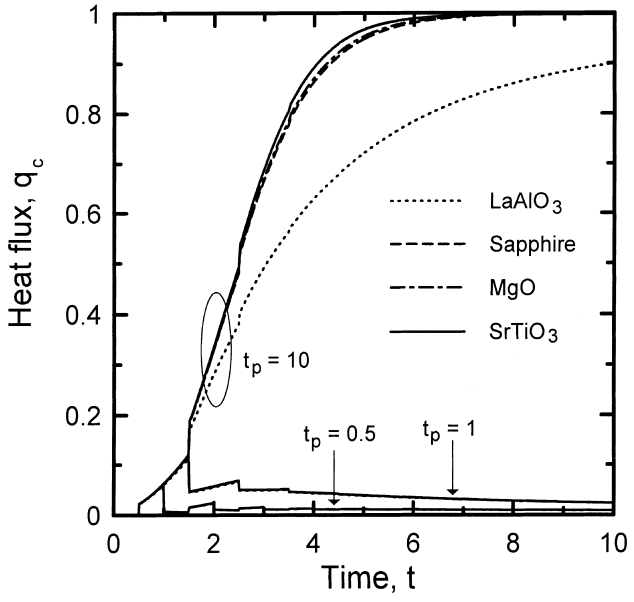

Fig. 11. Interface heat flux versus time with various durations.

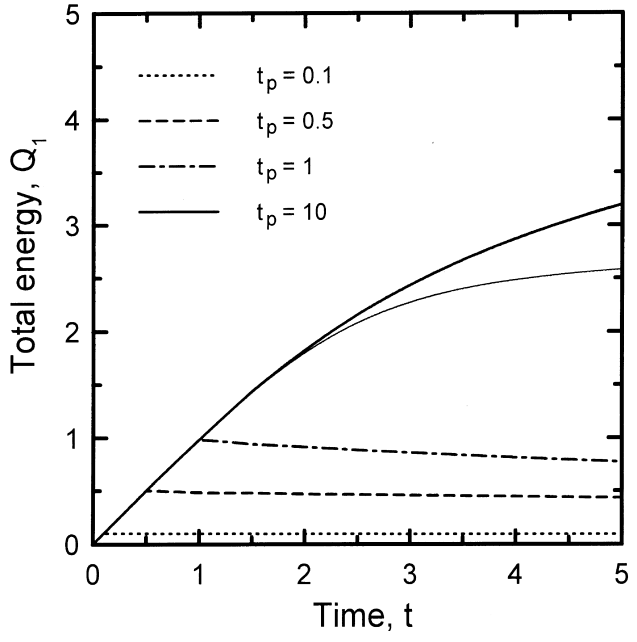

Fig. 12. Comparison of parabolic and hyperbolic film total energy versus time with various durations for substrate $LaAlO_3$. The light and dark lines represent the parabolic and hyperbolic solutions, respectively.

implies that when the duration is shorter than 2, the average film temperatures obtained for both heat transfer models coincide. The film temperature at the interface predicted by parabolic approximation instantaneously, and then continuously builds by the imposed surface heat flux. However, for the hyperbolic model, the imposed film surface heat flux builds to the film surface temperature, but does not build the film interface temperature until the wave front reaches the interface. That accounts for the total energy in the film for the parabolic solution being lower than that predicted by the hyperbolic equation for time scales larger than 2 when the duration is longer than 2. The physical time scale to correspond to a dimensionless duration value of 2 is four times that of Y–Ba–Cu–O relaxation time.

5. Conclusions

By applying the thermal wave theory, this study numerically analyzes heat conduction in the film and substrate composites under an imposed surface heat flux on the exterior film surface. The results demonstrate that the reflection and transmission occur when the wave front impacts the contact surface of the dissimilar material. The relative energy concentration in the reflected wave front and transmitted wave front varies with the substrate properties and interface conditions. The interface thermal resistance restricts the energy transmitted across the interface to the substrate, the energy stays in the film and ultimately increases the film temperature. The bare film approximation which ignores the substrate and interface resistance effects, significantly underestimates the film temperature.

In addition, the heat conduction for Y–Ba–Cu–O film deposited on several common substrates is examined. The radiation-boundary-condition at the interface where the thermal flow across the interface is proportional to the difference of the fourth power of the temperature on each side of the interface, is employed to take into account the interface resistance. The heat transfer in the film is nearly independent of those deposited substrates for short surface heat pulse duration in spite of the different thermal properties among those substrates. The substrate dependence gives rise to the film temperature using substrate $LaAlO_3$ being higher than that using other substrates when a longer surface heat pulse duration is imposed. Moreover, the thermal wave model predicts a significantly different film temperature distribution in small time scales than those predicted by the Fourier's diffusion model. Nevertheless, the average film temperature obtained for both equations coincides when the dimensionless duration of the surface heat pulse is shorter than 2, because the interface resistance magnitude is almost equivalent to that of an adiabatic condition. For duration longer than 2, the hyperbolic solution predicts a higher average film temperature than that predicted by the parabolic equation. Using $LaAlO_3$ substrate requires longer time scales than using other substrates for the solutions obtained from the diffusion model to coincide with the thermal wave model.

Acknowledgements

The authors would like to thank the National Science Council of Taiwan, ROC for financially supporting this research under Contract No. NSC 88-2218-E-009-003. Dr. J.P. Wu is also appreciated for his valuable discussions.

References

[1] Flik MI, Phelan PE, Tien CL. Thermal model for the bolometric response of high T_c superconducting film to optical pulses. Cryogenics 1990;30:1118–28.
[2] Chen RC, Wu JP, Chu HS. Bolometric response of high-T_c superconducting detectors to optical pulses and continuous waves. ASME J Heat Transfer 1995;117:366–72.
[3] Phelan PE. Thermal response of thin-film high T_c superconductors to modulated irradiation. J Thermophysics Heat Transfer 1995;9:397–402.
[4] Phelan PE. Application of diffuse mismatch theory to the prediction of thermal boundary resistance in thin-film high-T_c superconductors. ASME J Heat Transfer 1998;120:37–43.
[5] Wu JP, Chu HS. Substrate effects on intrinsic thermal stability and quench recovery for thin-film superconductors. Cryogenics 1996;36:925–35.
[6] Bertman B, Sandiford DJ. Second sound in solid helium. Scientific American 1970;222:92–101.
[7] Maurer MJ, Thompson HA. Non-Fourier effects at high heat flux. ASME J Heat Transfer 1973;95:284–6.
[8] Vedavarz A, Kumar S, Moallemi MK. Significance of Non-Fourier heat waves in conduction. ASME J Heat Transfer 1994;116:221–4.
[9] Guo ZY, Xu YS. Non-Fourier heat conduction in IC chip. ASME J Heat Transfer 1995;117:174–7.
[10] Cattaneo C. A form of heat conduction equation which eliminates the paradox of instantaneous propagation. Compute Rendus 1958;247:431–3.
[11] Vernotte P. Les paradoxes de la theorie continue de l'equation de la chaleur. Compute Rendus 1958;246:3145–55.
[12] Joseph DD, Preziosi L. Heat wave. Rev Modern Phys 1989;61: 41–73.
[13] Chester M. Second sound in solid. Physical Rev 1963;131:2013–5.
[14] Maurer MJ. Relaxation model for heat conduction in metals. J Appl Phys 1969;40:5123–30.
[15] Francis HP. Thermo-mechanical effects in elastic wave propagation: a survey. J Sound Vibration 1972;21:181–92.
[16] Sieniutycz S. The variational principles of classical type for non-coupled nonstationary irreversible transport processes with convective motion and relaxation. Internat J Heat Mass Transfer 1977;20:1221–31.
[17] Kaminski W. Hyperbolic heat conduction equation for materials with a nonhomogeneous inner structure. ASME J Heat Transfer 1990;112:555–60.

[18] Sahoo RK. Propagation of thermal waves with lateral heat transfer. Cryogenics 1994;34:203–12.
[19] Heremans J, Morelli DT, Smith GW, Strite SC. Thermal and electronic properties of rare-earth $Ba_2Cu_3O_x$ superconductors. Phys Rev B 1988;37:1604–10.
[20] Lang M, Lechner T, Riegel S, Steglich F, Weber G, Kim TJ, Lüthi B, Wolf B, Rietschel H, Wilhelm M. Thermal expansion, sound velocities, specific heat and pressure derivative of T_c in $YBa_2Cu_3O_7$. Zeitschrift fur Physik B 1988;69:459–63.
[21] Mitra K, Kumar S, Vedavarz A, Moallemi MK. Experimental evidence of hyperbolic heat conduction in processed meat. ASME J Heat Transfer 1995;117:568–73.
[22] Özisik MN, Tzou DY. On the wave theory in heat conduction. ASME J Heat Transfer 1994;116:526–35.
[23] Tzou DY. On the thermal shock wave induced by a moving source. ASME J Heat Transfer 1989;111:232–8.
[24] Braginski AI, Forrester MG, Talvacchio J. Progress toward understanding the mechanism of optical detection by high-temperature superconductors. Proc Internat Superconductivity Electronics Conf 1989.
[25] Frenkel A, Saifi MA, Venkatesan T, England P, Wu XD, Inam A. Optical response of non-granular high T_c $Y_1Ba_2Cu_3O_{7-x}$ superconducting thin film. J Appl Phys 1990;67:3054–68.
[26] Wiggert DC. Analysis of early-time transient heat conduction by method of characteristics. ASME J Heat Transfer 1977;99:35–40.
[27] Glass DE, Özisik MN, Kim WS. Hyperbolic Stefan problem with applied surface heat flux and temperature-dependent thermal conductivity. Numer Heat Transfer A 1990;18:503–16.
[28] Bai C, Lavine AS. Hyperbolic heat conduction in a superconducting film. ASME/JSME Thermal Eng Proc 1991;4:87–92.
[29] Bai C, Lavine AS. On hyperbolic heat conduction and the second law of thermodynamics. ASME J Heat Transfer 1995;117:256–63.
[30] Tan ZM, Yang WJ. Heat transfer during asymmetrical collision of thermal waves in a thin film. Internat J Heat Mass Transfer 1997;40:3999–4006.
[31] Kronberg AE, Benneker AH, Westerterp KR. Notes on wave theory in heat conduction: a new boundary condition. Internat J Heat Mass Transfer 1998;41:127–37.
[32] Glass DE, Özisik MN, Vick B. Non-Fourier effects on transient temperature resulting from periodic on-off heat flux. Internat J Heat Mass Transfer 1987;30:1623–31.
[33] Yuen WW, Lee SC. Non-Fourier heat conduction in a semi-infinite solid subjected to oscillatory surface thermal disturbances. ASME J Heat Transfer 1989;111:178–81.
[34] Tang DW, Araki N. Non-Fourier heat conduction in a finite medium under periodic surface disturbance. Internat J Heat Mass Transfer 1996;39:1585–90.
[35] Gembarovic J, Majernik V. Non-Fourier propagation of heat pulses in finite medium. Internat J Heat Mass Transfer 1988;31:1073–80.
[36] Glass DE, Tamma KK, Railkar SB. Hyperbolic heat conduction with convection boundary conditions and pulse heating effects. J Thermophysics 1990;5:110–6.
[37] Kim WS, Hector Jr. LG, Özisik MN. Hyperbolic heat conduction due to axisymmetric continuous or pulsed surface heat sources. J Appl Phys 1990;68:5478–85.
[38] Wu JP, Shu YP, Chu HS. Transient heat transfer phenomenon of two-dimensional hyperbolic heat conduction problem. Numer Heat Transfer A 1998;33:635–52.
[39] Frankel JI, Vick B, Özisik MN. General formulation and analysis of hyperbolic heat conduction in composite media. Internat J Heat Mass Transfer 1987;30:1293–305.
[40] Little WA. The transport of heat between dissimilar solid at low temperature. Can J Phys 1959;37:334–49.
[41] Swartz ET, Pohl RO. Thermal boundary resistance. Rev Modern Phys 1989;61:605–68.
[42] Yang HQ. Characteristics-based, high-order accurate and nonoscillatory numerical method for hyperbolic heat conduction. Numer Heat Transfer B 1990;18:221–41.
[43] Yeung WK, Lam TT. A numerical scheme or non-Fourier heat conduction, part I: one-dimensional problem formulation and applications. Numer Heat Transfer B 1998;33:215–33.
[44] Michael PC, Trefny JU, Yarar B. Thermal transport properties of single crystal lanthanum Aluminate. J Appl Phys 1992;72:107–9.
[45] Touloukian YS, Dewitt DP. Thermophysical Properties of Matter. New York: IFI/Plenum, 1981.